

# ANN (Artificial Neural Network) Controlled Virtual Laboratory Design for NdFeB Magnet Production

Mustafa KARHAN\*, Musa Faruk ÇAKIR

**Abstract:** Magnets have an important place in electrical and electronic systems and applications nowadays. The developments in the field of magnets have also greatly expanded their usage areas. NdFeB magnets play active and important role in this development. In this study, design of virtual laboratory to be used for the production of nanocomposite NdFeB magnets has been realized. Maximum energy product ( $BH_{max}$ ) is an important value for permanent magnets. The high  $BH_{max}$  value in small volume for the magnets is a desired criterion. In the study, mathematical functions were created from the data related to  $B_r$  (permanent magnetism),  $H_c$  (magnetic coercivity),  $BH_{max}$ ,  $T_c$  (Curie temperature) and density obtained in the researches on different NdFeB alloys in the laboratory. Additionally,  $B_r$  functions were obtained by adding different additives (Co, Ti, Zr, Hf, V, Ta, Nb, Cr, W, Mo, Mn, Ni, Sb, Sn, Ge, Al, Bi) to the NdFeB magnets. A virtual laboratory is prepared with the created functions. The obtained results from the operation of the virtual laboratory system and the results obtained from Matlab Simulink and ANN (Artificial Neural Network) systems are compared. The designed and performed virtual laboratory system can be used both for industrial purposes and for educational purposes.

**Keywords:** ANN (Artificial Neural Network);  $BH_{max}$ ; nanocomposite; NdFeB; permanent magnet; virtual laboratory

## 1 INTRODUCTION

Permanent magnets have the ability to consistently release magnetic flux to the air gap of a magnetic circuit. The flux density may be regular, irregular, stable or variable in the time. The most important property for a permanent magnet is the maximum energy product ( $BH_{max}$ ). At the beginning of the century,  $BH_{max}$  values of natural magnets were 10 kJ/m<sup>3</sup>, while NdFeB magnets with a value of 400 kJ/m<sup>3</sup>  $BH_{max}$  are made today. Recently, the energy products of nanocomposite NdFeB hard magnets under laboratory conditions have increased to 1090 kJ/m<sup>3</sup> [1-4]. A remarkable effort has been made to enhance the magnetic and physical properties of NdFeB magnets. Ferromagnetic elements such as iron and cobalt are widely used. Sm-Co and Nd-Fe-B rare earth magnets have a technologically important place because they give a high  $BH_{max}$  value [1, 5]. Sintered NdFeB magnets can be added with small amounts of resistant elements (Ti, Zr, Hf, V, Ta, Nb, Cr, W, Mo, Mn, Ni, Sb, Sn, Ge, Al, Bi) to increase their coercivity [6-8]. In addition, the enhanced magnetic and physical properties make these magnets' thermal stability very good [9]. Ferromagnetic metals such as Co and Ni from the transition elements increase the magnetization and  $T_c$ , Curie temperature. Elements such as Mo, Nb, Ti, V, W which have higher melting temperature than non-magnetic metals and elements such as Sn, Ga, Al, Cu and Sn with low melting temperature inhibit the growth of grains with the phases that occur at the grain boundaries. They decrease the magnetic interaction between the grains and increase the strength. At the same time, permanent magnetization can be reduced by these non-magnetic phases [10-15]. As a result of many researches, the coercivity values of Nd-Fe-B permanent magnets have been increased by additive elements with high melting temperatures such as Nb, Mo, W, Ti [16, 17]. In order to obtain optimum magnetic and physical properties of the magnets, it is necessary to sinter and cool immediately between 650 °C and 1160 °C [18]. Sintering is a high temperature process by which material powders combine to one another by diffusion through the effect of temperature and gradually reduce the pore volume between

the powders [19]. In multicomponent systems, sintering temperature is set to the lower values of metal with low melting temperature. As the sintering temperature increases, sintering time decreases [20].

Composite materials are composed of two or more of the same or different types of materials combined at a macro level to collect the best properties of the materials in a new and single material. [21]. The nanocomposites are a new type of composite material containing mineral and an amount of nanosized mineral smaller than 10%.

Due to the wide surface area of the nano-sized particles used, mechanical, thermal and magnetic properties show improvements in positive direction. Due to these properties of composite materials, they play active and important role in the production of NdFeB magnets. NdFeB magnets have many properties when they are produced as composites. The high magnetism properties in small volume are at the top of these properties. Significant studies on NdFeB magnets still continue. It is tried to get higher values of magnetism properties by adding various additives.

The obtained data in the production of these magnets have been used for the system we have simulated. In different alloy magnets, the mathematical functions of the magnetic properties which are important for the magnets have been obtained. These functions are  $BH_{max}$ ,  $H_c$  and  $B_r$  functions. The virtual laboratory system was designed and performed using the obtained function, MATLAB Simulink and ANN (Artificial Neural Network). There are studies using ANN on MATLAB/Simulink platform in many fields of engineering [22-26]. In this study, ANN controlled virtual laboratory on MATLAB/Simulink platform is presented at the intersection of electrical electronics engineering, material engineering, and software engineering.

The data we used to obtain mathematical functions was taken from the work of United States patent number 5-183-516. [27, 28].

## 2 MATHEMATICAL FUNCTIONS OF NANOCOMPOSITE NdFeB ALLOYS

### 2.1 Data of Mathematical Functions

Mathematical functions are needed to be used when preparing a virtual laboratory.  $BH_{\max}$ ,  $H_c$  and  $B_r$  functions must be obtained using the following data for alloy 15Nd-(85-x)Fe-xB. These functions form the basis of the virtual laboratory.

The effect of B (Boron) element on the magnetic properties of NdFeB magnets is shown in Tab. 1.

**Table 1** The Data of 15Nd-(85-x)Fe-xB alloy [27]

| Alloy Name: 15Nd-(85-x)Fe-xB |            |             |                    |
|------------------------------|------------|-------------|--------------------|
| % B                          | $B_r$ / kG | $H_c$ / kOe | $BH_{\max}$ / MGoe |
| 0                            | 0,0        | 0,00        | 0                  |
| 2                            | 7,5        | 1,3         | 4,1                |
| 3                            | 10,4       | 1,8         | 7,0                |
| 4                            | 10,8       | 2,8         | 13,4               |
| 6                            | 13,0       | 8,0         | 36,5               |
| 7                            | 12,9       | 8,2         | 36,0               |
| 8                            | 12,1       | 7,3         | 32,1               |
| 10                           | 11,9       | 8,0         | 31,9               |
| 12                           | 10,5       | 8,2         | 25,2               |
| 17                           | 8,7        | 7,6         | 17,6               |
| 23                           | 6,8        | 11,3        | 10,9               |
| 30                           | 4,2        | 10,7        | 4,0                |
| 32                           | 3,0        | 10,2        | 1,8                |

The effect of Nd (neodymium) element on the magnetic properties of NdFeB magnets is shown in Tab. 2.

**Table 2** The Data of xNd-(92-x)Fe-8B alloy [27]

| Alloy Name: xNd-(92-x)Fe-8B |            |             |                    |
|-----------------------------|------------|-------------|--------------------|
| % Nd                        | $B_r$ / kG | $H_c$ / kOe | $BH_{\max}$ / MGoe |
| 6                           | 0          | 0           | 0                  |
| 13                          | 13,1       | 4,8         | 29,3               |
| 14                          | 12,8       | 7,8         | 36,5               |
| 17                          | 11,6       | 9,2         | 31,1               |
| 19                          | 10,9       | 11,4        | 28,0               |
| 25                          | 5,8        | 12,6        | 8,8                |
| 35                          | 1,9        | 14,6        | $\leq 1$           |

**Table 3** The Data of 15Nd-(77-x)Fe-8B-zM alloy [27]

| Alloy Name: 15Nd-(77-x)Fe-8B-zM                         |         |         |         |        |         |         |         |        |
|---|---------|---------|---------|--------|---------|---------|---------|--------|
| $B_r$ values when added additives, $M$ = Added material |         |         |         |        |         |         |         |        |
| % M   | Ti / kG | Zr / kG | Hf / kG | V / kG | Ta / kG | Nb / kG | Cr / kG | W / kG |
| 0   | 12,0    | 12,0    | 12,0    | 12,0   | 12,0    | 12,0    | 12,0    | 12,0   |
| 0,5   | 12,3    | 11,9    | 11,9    |        | 11,6    |         | 11,6    | 11,6   |
| 1   | 12,0    | 11,7    | 11,7    | 11,5   | 11,6    | 11,9    | 11,4    | 11,4   |
| 1,5   | 11,8    | 11,4    | 11,4    |        |         |         |         |        |
| 2   | 11,2    | 10,7    | 10,7    | 11,0   | 11,4    | 11,7    | 10,9    | 11,0   |
| 3   | 8,7     | 9,2     | 9,2     | 10,3   |         |         |         |        |
| 4   | 6,0     | 7,5     | 7,5     | 9,8    | 10,5    | 11,0    | 9,5     | 9,8    |
| 5   | 2,4     | 5,3     | 5,3     |        |         |         |         |        |
| 6   |         | 2,2     | 2,2     | 8,5    | 9,5     | 10,2    | 7,6     | 8,0    |
| 7   |         |         |         |        |         |         |         |        |
| 8   |         |         |         | 7,0    | 8,4     | 9,4     | 5,2     | 5,9    |
| 9   |         |         |         |        | 5,7     | 7,5     | 9,0     |        |
| 10  |         |         |         |        | 3,5     | 6,0     | 8,2     | 2,3    |
| 11  |         |         |         |        |         | 3,7     |         | 3,5    |
| 12  |         |         |         |        |         | 5,4     |         |        |

When additives are added to an alloy, the resulting residual magnetism in the alloy ( $B_r$ ) the data used to obtain the required functions in order to observe the changes are given in Tab. 3 and Tab. 4.

**Table 4** The Data of 15Nd-(77-x)Fe-8B-zM alloy [27]

| $B_r$ values when added additives<br>$M$ = Added material |      |      |      |      |      |      |      |
|---|------|------|------|------|------|------|------|
| % M   | Mn   | Ni   | Sb   | Sn   | Ge   | Al   | Bi   |
| 0,0   | 12,0 | 12,0 | 12,0 | 12,0 | 12,0 | 12,0 | 12,0 |
| 0,5   | 11,3 | 11,8 |      |      | 11,4 | 12,1 |      |
| 1,0   | 10,7 | 11,9 | 9,2  | 10,0 | 11,0 | 11,4 | 11,7 |
| 1,5   |      |      |      |      |      |      |      |
| 2,0   | 9,9  | 11,6 | 6,1  | 7,8  | 10,3 | 10,9 | 11,4 |
| 3,0   |      |      |      |      | 5,5  |      |      |
| 4,0   | 9,1  | 11,1 | 2,9  | 3,5  | 8,4  | 9,6  | 10,4 |
| 5,0   |      |      |      |      |      |      | 10,0 |
| 6,0   | 8,7  | 10,2 |      |      | 6,5  | 8,4  |      |
| 7,0   |      |      |      |      |      |      |      |
| 8,0   | 8,2  | 9,2  |      |      | 3,5  | 6,4  |      |
| 9,0   |      |      |      |      |      |      |      |
| 10,0  | 7,3  | 8,0  |      |      |      |      | 3,4  |

### 2.2 $B_r$ Functions

$B_r$  functions are directly effective as a multiplier in determining  $BH_{\max}$  for alloys. It is a common value for different alloy structures. It is also used for magnet characterization for different magnet alloys. These are functions of residual magnetism when % M additives ( $M$  = Ti, Zr, Hf, V, Ta, Nb, Cr, W, Mo, Mn, Ni, Sb, Sn, Ge, Al, Bi) are added to the 15Nd-Fe-8B-xM alloy from the obtained alloys and they are pressed in 10 kOe magnetic field. The obtained  $B_r$  functions for the different additives are given in Eqs. (1) to (15).

Alloy Formula: 15 Nd-(77-x)Fe-8B-xM  
( $M$  = Ti, Zr, Hf, V, Ta, Nb, Cr, W, Mo, Mn, Ni, Sb, Sn, Ge, Al, Bi).

$$FB_r(\text{Ti}) = -0,02969 \cdot x^6 + 0,4061 \cdot x^5 - 2,03 \cdot x^4 + 4,555 \cdot x^3 - 5,048 \cdot x^2 + 2,181 \cdot x + 12 \quad (1)$$

$$FB_r(\text{Zr}) = 0,002656 \cdot x^6 - 0,04875 \cdot x^5 + 0,3254 \cdot x^4 - 0,9443 \cdot x^3 + 0,8405 \cdot x^2 - 0,4438 \cdot x + 12 \quad (2)$$

$$FB_r(\text{Hf}) = 0,002656 \cdot x^6 - 0,04875 \cdot x^5 + 0,3254 \cdot x^4 - 0,9443 \cdot x^3 + 0,8405 \cdot x^2 - 0,4438 \cdot x + 12 \quad (3)$$

$$FB_r(\text{V}) = 2,769 \times 10^{-5} \cdot x^6 + 0,0005505 \cdot x^5 - 0,004751 \cdot x^4 + 0,02434 \cdot x^3 - 0,8509 \cdot x^2 - 0,4179 \cdot x + 12 \quad (4)$$

$$FB_r(\text{Ta}) = 9,06 \times 10^{-5} \cdot x^6 - 0,003284 \cdot x^5 + 0,04315 \cdot x^4 - 0,02561 \cdot x^3 + 0,6518 \cdot x^2 - 0,8792 \cdot x + 12 \quad (5)$$

$$FB_r(\text{Nb}) = 1,69410 \times 10^{-5} \cdot x^6 - 0,0006699 \cdot x^5 + 0,04315 \cdot x^4 - 0,04354 \cdot x^3 + 0,03859 \cdot x^2 - 0,1106 \cdot x + 12 \quad (6)$$

$$FB_r(\text{Cr}) = 0,0001103 \cdot x^6 - 0,003334 \cdot x^5 + 0,03832 \cdot x^4 - 0,209 \cdot x^3 + 0,4847 \cdot x^2 - 0,9313 \cdot x + 11,99 \quad (7)$$

$$FB_r(\text{W}) = 7,928 \times 10^{-5} \cdot x^6 - 0,002619 \cdot x^5 + 0,03346 \cdot x^4 - 0,2043 \cdot x^3 + 0,5359 \cdot x^2 - 0,9768 \cdot x + 11,99 \quad (8)$$

$$FB_r(\text{Mo}) = -5,397 \times 10^{-5} \cdot x^6 + 0,001243 \cdot x^5 - 0,00874 \cdot x^4 + 0,01178 \cdot x^3 + 0,01955 \cdot x^2 - 0,4964 \cdot x + 12,01 \quad (9)$$

$$FB_r(\text{Mn}) = 9,515 \times 10^{-6} \cdot x^6 + 0,0002207 \cdot x^5 - 0,0008097 \cdot x^4 - 0,02473 \cdot x^3 + 0,3136 \cdot x^2 - 1,579 \cdot x + 12 \quad (10)$$

$$FB_r(\text{Ni}) = -1,097 \times 10^{-5} \cdot x^6 + 0,0001658 \cdot x^5 + 0,0004199 \cdot x^4 - 0,01631 \cdot x^3 + 0,0453 \cdot x^2 - 0,2002 \cdot x + 11,98 \quad (11)$$

$$FB_r(\text{Sb}) = 0,1 \cdot x^2 - 2,74 \cdot x + 12,01 \quad (12)$$

$$FB_r(\text{Ge}) = 0,002315 \cdot x^5 + 0,0429 \cdot x^4 - 0,279 \cdot x^3 + 0,7251 \cdot x^2 - 1,489 \cdot x + 12 \quad (13)$$

$$FB_r(\text{Al}) = -0,0001244 \cdot x^6 + 0,004023 \cdot x^5 - 0,04979 \cdot x^4 + 0,2833 \cdot x^3 - 0,7224 \cdot x^2 + 0,03448 \cdot x + 12,05 \quad (14)$$

$$FB_r(\text{Bi}) = 0,008333 \cdot x^4 + 0,075 \cdot x^3 + 0,1667 \cdot x^2 - 0,4 \cdot x + 12 \quad (15)$$

### 2.3 $BH_{\max}$ and $H_c$ Functions

From the alloys formed to observe the effects of Nd and B; The effect of B with 15Nd-(85-x)Fe-xB and the effect of Nd with xNd-(92-x)Fe-8B alloy were investigated and Br and Hc functions were established for % B change and % Nd change. The obtained  $B_r$ ,  $H_c$  and  $BH_{\max}$  functions for 15Nd-(85-x)Fe-xB are given in Eqs. (16) to (18). The obtained  $B_r$ ,  $H_c$  and  $BH_{\max}$  functions for xNd-(92-x)Fe-8B are given in Eqs. (19) to (21).

Alloy Formula: 15Nd-(85-x)Fe-xB

$$FB_r(\text{B}) = 9,754 \times 10^{-6} \cdot x^5 - 0,0009972 \cdot x^4 + 0,03813 \cdot x^3 - 0,6705 \cdot x^2 + 4,959 \cdot x + 0,05367 \quad (16)$$

$$FH_c(\text{B}) = -8,322 \times 10^{-5} \cdot x^4 + 0,006099 \cdot x^3 - 0,1613 \cdot x^2 + 2,004 \cdot x - 1,316 \quad (17)$$

$$FBH_{\max}(\text{B}) = -0,0001754 \cdot x^4 + 0,02022 \cdot x^3 - 0,7541 \cdot x^2 + 9,474 \cdot x - 6,858 \quad (18)$$

Alloy Formula: xNd-(92-x)Fe-8B

$$FB_r(\text{Nd}) = -0,0001578 \cdot x^4 + 0,01715 \cdot x^3 - 0,6637 \cdot x^2 + 10,21 \cdot x - 40,84 \quad (19)$$

$$FH_c(\text{Nd}) = -8,242 \times 10^{-5} \cdot x^3 - 0,01436 \cdot x^2 + 1,217 \cdot x - 6,966 \quad (20)$$

$$FBH_{\max}(\text{Nd}) = 0,00026 \cdot x^4 - 0,006882 \cdot x^3 - 0,4002 \cdot x^2 + 13,11 \cdot x - 63,16 \quad (21)$$

Using the above functions, the following virtual laboratory was prepared. Screen shot of the developed virtual laboratory software is given in Fig. 1.

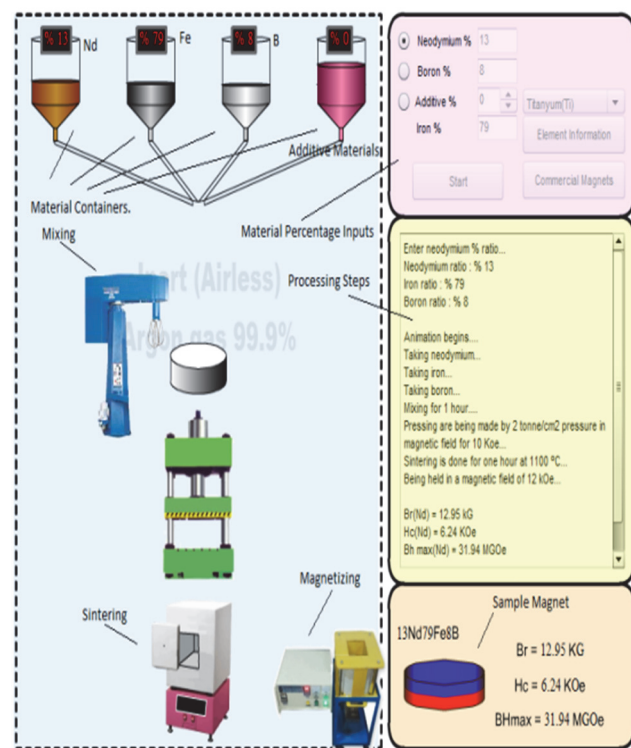


Figure 1 Screen shot of the developed virtual laboratory software [1]

When we want to produce magnet based on Nd element, when we input Nd value as % in our virtual laboratory, the system works and the alloy formula and  $BH_{\max}$  values of the sample are obtained. We can obtain NdFeB alloys by doing the same steps for element B. When we select the additive and enter the % ratio in our virtual laboratory we get the residual magnetization value of the alloy 15Nd-Fe-8B-xM to investigate the effect of additives on the residual magnetism ( $B_r$ ) of the NdFeB magnet ( $M = \text{Additives}$ ).

Today's commercial magnets are also included in the virtual lab.  $B_r$ ,  $BH_{\max}$  and commercial magnets can be selected according to operating temperatures. We can also investigate the chemical and physical properties of all the elements.

### 3 CONTROLLING OF VIRTUAL LABORATORY WITH ARTIFICIAL NEURAL NETWORK

The block diagram of the controlling of virtual laboratory with artificial neural network (ANN) is given below (Fig. 2).

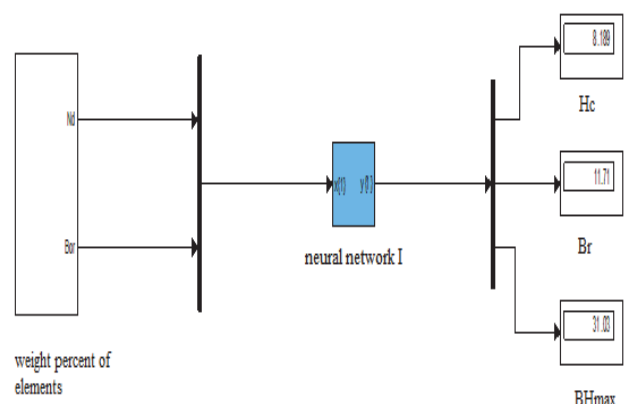


Figure 2 The block diagram of the controlling of virtual laboratory

5-layer ANN block and internal structure are shown below (Fig. 3) [29, 30].

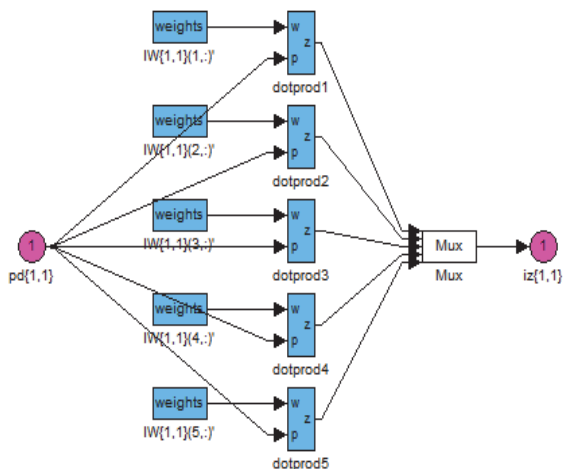


Figure 3 5-layer ANN block. [24, 25]

The graphs of  $B_r$ ,  $H_c$  and  $BH_{max}$  for Nd and B changes are shown below (Fig. 4 and Fig. 5) when the above ANN block diagram is run for all input values.

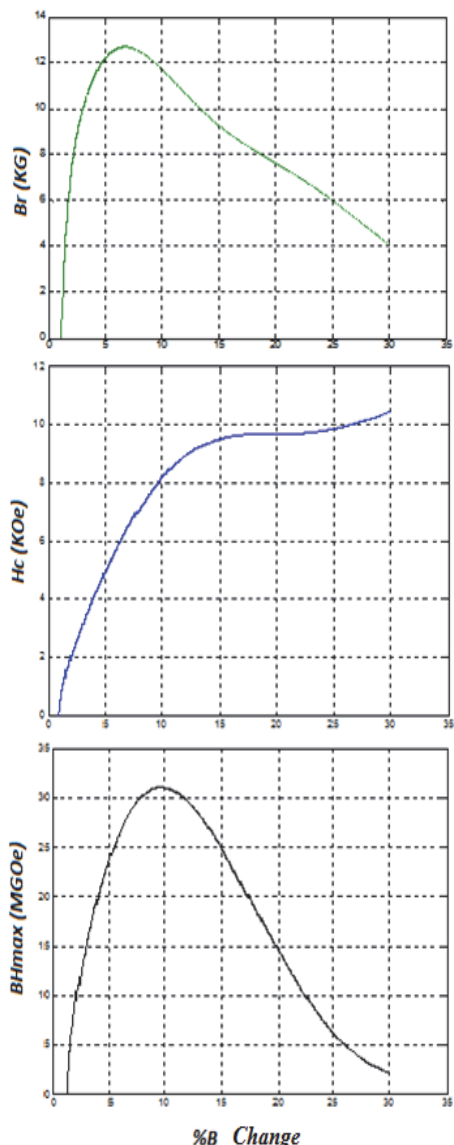


Figure 4  $B_r$ ,  $H_c$  and  $BH_{max}$  graphs versus % B change in the results of ANN

When the above chart is analysed, the highest value of the  $BH_{max}$  of the magnet is about 10% of the B (Boron) value. The graph of magnetic property which is important for the magnet ( $BH_{max}$ ,  $B_r$  and  $H_c$ ) should be examined in detail. In some magnets, the coercivity ( $H_c$ ) may be more important than  $BH_{max}$ . In these cases, the graphical values of the coercivity ( $H_c$ ) should be chosen in the most ideal way.

When the below chart is analysed, the highest value of the  $BH_{max}$  of the magnet is about 15% of the Nd (Neodymium) value. If the  $B_r$  value is more important than  $BH_{max}$ , the Nd value should be around 10-15%. Which properties of the magnets produced are more important should be determined and the % Nd value should be adjusted. The obtained values using by ANN provided a more robust and reliable virtual laboratory.

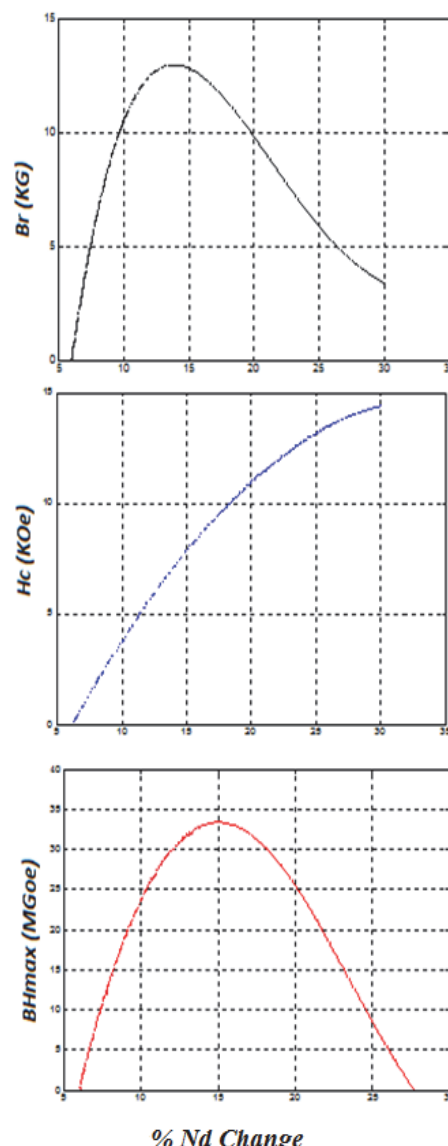


Figure 5  $B_r$ ,  $H_c$  and  $BH_{max}$  graphs versus % Nd change in the results of ANN

#### 4 CONCLUSION AND SUGGESTIONS

In order to test the prepared virtual laboratory, studies with the same values as the environment values (mixing time, pressure, applied magnetic field, sintering temperature and sintering time) in the preparation of the

data we used. The following results were obtained when we compared the results. Comparison of all results is given in Tab. 5.

The algorithm, which was followed when performing experiments in the real laboratory environment, was also used in preparing the virtual laboratory environment. In this way it is possible to compare actual test results with software results. The values of results of virtual labs are close to the averages of ANN results with real experiments. The results in each section are very close together. Through virtual laboratory, it is possible to make magnet

experiments by mixing materials in desired rate. The software can simulate interim values for the currently manufactured magnet alloys. In this way, both the time spent in the production of samples and the material costs are eliminated.

By means of the prepared virtual laboratory, we can obtain the properties of the produced commercial magnets. In this section you can see whether there is a magnet in the desired properties. The properties of the magnet you need are also available from this part. In addition, physical and chemical properties of the used elements can be studied.

**Table 5 Comparison of virtual laboratory results, artificial neural networks and other study results**

| Comparison of Laboratory Results                                |   |   |
|---|---|---|
| Virtual Laboratory  | ANN   | Simulink  |
| Nd = 20, B = 8 20Nd72Fe8B Alloy                                 |   |   |
| $B_r = 10.15$ kG<br>$H_c = 10.97$ kOe<br>$BH_{max} = 25.5$ MGOe | $B_r = 9.843$ kG<br>$H_c = 10.9$ kOe<br>$BH_{max} = 25.58$ MGOe   | $B_r = 9.832$ kG<br>$H_c = 10.96$ kOe<br>$BH_{max} = 25.55$ MGOe  |
| Nd = 10, B = 8 10Nd82Fe8B Alloy                                 |   |   |
| $B_r = 10.48$ kG<br>$H_c = 3.68$ kOe<br>$BH_{max} = 23.63$ MGOe | $B_r = 10.51$ kG<br>$H_c = 3.717$ kOe<br>$BH_{max} = 23.61$ MGOe  | $B_r = 10.46$ kG<br>$H_c = 3.684$ kOe<br>$BH_{max} = 23.67$ MGOe  |
| Nd = 15, B = 10 15Nd75Fe10B Alloy                               |   |   |
| $B_r = 11.72$ kG<br>$H_c = 7.86$ kOe<br>$BH_{max} = 30.93$ MGOe | $B_r = 11.71$ kG<br>$H_c = 8.189$ kOe<br>$BH_{max} = 31.03$ MGOe  | $B_r = 11.7$ kG<br>$H_c = 8.118$ kOe<br>$BH_{max} = 30.94$ MGOe   |
| Nd = 17, B = 8 17Nd75Fe8B Alloy                                 |   |   |
| $B_r = 12.16$ kG<br>$H_c = 9.16$ kOe<br>$BH_{max} = 31.95$ MGOe | $B_r = 11.99$ kG<br>$H_c = 9.156$ kOe<br>$BH_{max} = 32.09$ MGOe  | $B_r = 12$ kG<br>$H_c = 9.159$ kOe<br>$BH_{max} = 31.99$ MGOe     |
| Nd = 7, B = 8 7Nd85Fe8B Alloy                                   |   |   |
| $B_r = 3.61$ kG<br>$H_c = 0.82$ kOe<br>$BH_{max} = 7.26$ MGOe   | $B_r = 3.604$ kG<br>$H_c = 0.7575$ kOe<br>$BH_{max} = 7.359$ MGOe | $B_r = 3.612$ kG<br>$H_c = 0.8205$ kOe<br>$BH_{max} = 7.287$ MGOe |
| Nd = 27, B = 8 27Nd65Fe8B Alloy                                 |   |   |
| $B_r = 5.75$ kG<br>$H_c = 13.8$ kOe<br>$BH_{max} = 1.78$ MGOe   | $B_r = 4.685$ kG<br>$H_c = 13.78$ kOe<br>$BH_{max} = 2.012$ MGOe  | $B_r = 4.695$ kG<br>$H_c = 13.77$ kOe<br>$BH_{max} = 1.812$ MGOe  |
| Nd = 15, B = 15 15Nd70Fe15B Alloy                               |   |   |
| $B_r = 9.18$ kG<br>$H_c = 8.82$ kOe<br>$BH_{max} = 24.94$ MGOe  | $B_r = 9.273$ kG<br>$H_c = 9.491$ kOe<br>$BH_{max} = 24.94$ MGOe  | $B_r = 9.294$ kG<br>$H_c = 9.487$ kOe<br>$BH_{max} = 24.94$ MGOe  |
| Nd = 15, B = 20 15Nd65Fe20B Alloy                               |   |   |
| $B_r = 7.73$ kG<br>$H_c = 9.72$ kOe<br>$BH_{max} = 14.67$ MGOe  | $B_r = 7.635$ kG<br>$H_c = 9.673$ kOe<br>$BH_{max} = 14.59$ MGOe  | $B_r = 7.602$ kG<br>$H_c = 9.82$ kOe<br>$BH_{max} = 14.68$ MGOe   |
| Nd = 15, B = 25 15Nd60Fe25B Alloy                               |   |   |
| $B_r = 6.47$ kG<br>$H_c = 10.76$ kOe<br>$BH_{max} = 6.1$ MGOe   | $B_r = 6.006$ kG<br>$H_c = 9.847$ kOe<br>$BH_{max} = 6.235$ MGOe  | $B_r = 6.074$ kG<br>$H_c = 9.848$ kOe<br>$BH_{max} = 6.101$ MGOe  |
| Nd = 25 B = 8 25Nd67Fe8B Alloy                                  |   |   |
| $B_r = 6.7$ kG<br>$H_c = 13.19$ kOe<br>$BH_{max} = 8.49$ MGOe   | $B_r = 5.91$ kG<br>$H_c = 13.17$ kOe<br>$BH_{max} = 8.503$ MGOe   | $B_r = 5.926$ kG<br>$H_c = 13.17$ kOe<br>$BH_{max} = 8.544$ MGOe  |

## 5 REFERENCES

- [1] Çakır, M. F., Tarımer, İ., & Gürdal, O. (2014). Designing a virtual laboratory for simulating to production of nanocomposite NdFeB magnets. *TEM Journal*, 3(1), 8-12.
- [2] Crangle, J. (1977). *The Magnetic Properties of Solids*. Edward Arnold, London.
- [3] Yalçın, H. & Gürü, M. (2002). *Malzeme Bilgisi*. Palme Yayınevi.
- [4] Shandong, L., Yaodong, D., Gu, B. X., Zongjun, T., & Youwei, D. (2002). Effect of amorphous grain boundaries on the magnetic properties of B-rich nanocomposite permanent magnets. *Journal of alloys and compounds*, 339(1-2), 202-206. [https://doi.org/10.1016/S0925-8388\(01\)01992-2](https://doi.org/10.1016/S0925-8388(01)01992-2)
- [5] Corner, W. D. (1988). Permanent magnets. *Physics in Technology*, 19(4), 158.
- [6] Sagawa, M., Fujimura, S., Togawa, N., Yamamoto, H., & Matsuura, Y. (1984). New material for permanent magnets on a base of Nd and Fe. *Journal of Applied Physics*, 55(6), 2083-2087. <https://doi.org/10.1063/1.333572>
- [7] Herbst, J. F. (1991). R<sub>2</sub>Fe<sub>14</sub>B materials: Intrinsic properties and technological aspects. *Reviews of Modern Physics*, 63(4), 819. <https://doi.org/10.1103/RevModPhys.63.819>
- [8] Buschow, K. H. J. (1997). Magnetism and processing of permanent magnet materials. *Handbook of magnetic materials*, 10, 463-593. [https://doi.org/10.1016/S1567-2719\(97\)10008-7](https://doi.org/10.1016/S1567-2719(97)10008-7)
- [9] Sagawa, M., Tenaud, P., Vial, F., & Hiraga, K. (1990). High coercivity Nd-Fe-B sintered magnet containing vanadium with new microstructure. *IEEE transactions on magnetics*, 26(5), 1957-1959. <https://doi.org/10.1109/20.104581>

- [10] Vial, F., Joly, F., Nevalainen, E., Sagawa, M., Hiraga, K., & Park, K. T. (2002). Improvement of coercivity of sintered NdFeB permanent magnets by heat treatment. *Journal of magnetism and magnetic materials*, 242, 1329-1334. [https://doi.org/10.1016/S0304-8853\(01\)00967-2](https://doi.org/10.1016/S0304-8853(01)00967-2)
- [11] Croat, J. J., Herbst, J. F., Lee, R. W., & Pinkerton, F. E. (1984). Pr-Fe and Nd-Fe-based materials: A new class of high-performance permanent magnets. *Journal of Applied Physics*, 55(6), 2078-2082. <https://doi.org/10.1063/1.333571>
- [12] Yang, S., Song, X., Li, S., Liu, X., Tian, Z., Gu, B., & Du, Y. (2003). Effect of Cu and Ti additions on the microstructures and magnetic properties of Nd<sub>8</sub>Fe<sub>86</sub>B<sub>6</sub> nanocomposite magnets. *Journal of magnetism and magnetic materials*, 263(1-2), 134-140. [https://doi.org/10.1016/S0304-8853\(02\)01546-9](https://doi.org/10.1016/S0304-8853(02)01546-9)
- [13] Yan, A., Song, X., & Wang, X. (1997). Effect of minor intergranular additives on microstructure and magnetic properties of NdFeB based magnets. *Journal of magnetism and magnetic materials*, 169(1-2), 193-198. [https://doi.org/10.1016/S0304-8853\(96\)00713-5](https://doi.org/10.1016/S0304-8853(96)00713-5)
- [14] Rodewald, W. & Fernengel, W. (1988). Properties of sintered Nd-Fe-TM-B magnets. *IEEE Transactions on Magnetics*, 24(2), 1638-1640. <https://doi.org/10.1109/20.11555>
- [15] Gholamipour R. R., Beitollahi A., Marghusan V., Ohkubo V., & Hono, K. *Proc. of 19th International Workshop on Rare Earth Permanent Magnets and Their Applications*, 215-220.
- [16] Ishikawa, T., Hamada, Y., & Ohmori, K. (1989). Domain wall pinning by fine precipitates. *IEEE Transactions on Magnetics*, 25(5), 3434-3436. <https://doi.org/10.1109/20.42326>
- [17] Otani, Y., Miyajima, H., & Chikazumi, S. (1989). Large Barkhausen jumps observed in Nd-Fe-B sintered magnets at very low temperatures. *IEEE Transactions on Magnetics*, 25(5), 3431-3435. <https://doi.org/10.1109/20.42325>
- [18] Ragg, O. M. & Harris, I. R. (1997). A study of the effects of the addition of various amounts of Cu to sintered Nd-Fe-B magnets. *Journal of alloys and compounds*, 256(1-2), 252-257. [https://doi.org/10.1016/S0925-8388\(96\)02962-3](https://doi.org/10.1016/S0925-8388(96)02962-3)
- [19] Erdoğan, M. (1998). *Malzeme Bilimi ve Mühendislik Malzemeleri*. Nobel Yayınevi, Ankara.
- [20] Sümer, M. (2004). *Mekanik alaşımlama ile üretilen Fe-Fe<sub>3</sub>C kompozit malzemede mekanik özelliklerin araştırılması*. Yüksek Lisans Tezi, Gazi Üniversitesi Fen Bilimleri Enstitüsü, Ankara.
- [21] Şahin, Y. (2000). *Kompozit malzemelere giriş*. Gazi Kitapevi, Ankara.
- [22] Karamirad, M., Omid, M., Alimardani, R., Mousazadeh, H., & Heidari, S. N. (2013). ANN based simulation and experimental verification of analytical four-and five-parameters models of PV modules. *Simulation Modelling Practice and Theory*, 34, 86-98. <https://doi.org/10.1016/j.simpat.2013.02.001>
- [23] Malik, H. & Mishra, S. (2016). Artificial neural network and empirical mode decomposition based imbalance fault diagnosis of wind turbine using TurbSim, FAST and Simulink. *IET Renewable Power Generation*, 11(6), 889-902. <https://doi.org/10.1049/iet-rpg.2015.0382>
- [24] Rezk, H. & Hasaneen, E. S. (2015). A new MATLAB/Simulink model of triple-junction solar cell and MPPT based on artificial neural networks for photovoltaic energy systems. *Ain Shams Engineering Journal*, 6(3), 873-881. <https://doi.org/10.1016/j.asej.2015.03.001>
- [25] Bhattacharya, A. & Chakraborty, C. (2010). A shunt active power filter with enhanced performance using ANN-based predictive and adaptive controllers. *IEEE transactions on industrial electronics*, 58(2), 421-428. <https://doi.org/10.1109/TIE.2010.2070770>
- [26] Sharon, H., Jayaprakash, R., Sundaresan, A., & Karuppasamy, K. (2012). Biodiesel production and prediction of engine performance using SIMULINK model of trained neural network. *Fuel*, 99, 197-203. <https://doi.org/10.1016/j.fuel.2012.04.019>
- [27] Sagawa M., Furimuro S., & Matsuura Y. (1993). *Magnetic Materials and Permanent Magnets*. United States Patent, Patent. No: 5,183,516.
- [28] Sagawa, M., Furimuro, S., & Matsuura, Y. (1986). *Magnetic Materials and Permanent Magnets*. United States Patent, Patent. No: 4, 597, 938.
- [29] Beale, H. D., Demuth, H. B., & Hagan, M. T. (1996). *Neural network design*. Pws, Boston.
- [30] Fausett, L. (1994). *Fundamentals of neural networks: architectures, algorithms, and applications*. Prentice-Hall, Inc.

**Contact information:****Mustafa KARHAN, PhD**

(Corresponding author)

Cankiri Karatekin University, Electronics and Automation Department, Tasmescit Campus, 18100 Cankiri, Turkey  
E-mail: mustafakarhan@gmail.com**Musa Faruk ÇAKIR, PhD**Cankiri Karatekin University, Electronics and Automation Department, Tasmescit Campus, 18100 Cankiri, Turkey  
E-mail: mcakir@karatekin.edu.tr